Chapter 5

Ultra-Thin Plasma-Polymerized Functional Coatings for Biosensing: Polyacrylic Acid, Polystyrene and Their Co-Polymer

Paola Rivolo, Micaela Castellino,
Francesca Frascella and Serena Ricciardi

Additional information is available at the end of the chapter

http://dx.doi.org/10.5772/62899

Abstract

Recently, many efforts have been done to chemically functionalize sensors surface to achieve selectivity towards diagnostics targets, such as DNA, RNA fragments and protein tumoural biomarkers, through the surface immobilization of the related specific receptor. Especially, some kind of sensors such as microcantilevers (gravimetric sensors) and one-dimensional photonics crystals (optical sensors) able to couple Bloch surface waves are very sensitive. Thus, any kind of surface modifications devoted to functionalize them has to be finely controlled in terms of mass and optical characteristics, such as refractive index, to minimize the perturbation, on the transduced signal, that can affect the response sensitivity towards the detected target species.

In this work, the study and optimization of ultra-thin plasma polymers and copolymers, compatible with these constrains and obtained from the vapours of acrylic acid containing a carboxylic (–COOH) group and styrene (an aromatic molecule with a vinyl as substituent at the ring), are reported. The obtained plasma polyacrylic acid (PPAA), plasma polystyrene (PPST) and their copolymer (PPAA–ST), characterized through optical contact angle analysis (OCA), Fourier transform infrared (FTIR) spectroscopy in attenuated total reflection (ATR-FTIR), X-ray photoelectrons spectroscopy (XPS), and atomic force microscopy (AFM), are shown to match specific and critical requirements, such as low thickness (~40 nm) and refractive index (~1.5), high surface density of reactive groups (10^{15}–10^{16} COOH/cm^2), bio-antifouling properties where required, reproducibility, and chemical resistance and stability.

Keywords: plasma polymerization, acrylic acid, styrene, thin films, biosensing

1. Introduction

In the last decades, one of the most critical issues in biosensing devices was the proper surface chemical modification aimed to covalently immobilize a bioreceptor (e.g. a capture antibody) or probe (a single-stranded DNA, ss-DNA), able to selectively bind a target, by matching an antigen or an oligonucleotide sequence (DNA or RNA fragment) of interest for biodiagnostics, respectively [1–3]. Polymeric thin coatings, such as polyacrylic acid, polydi(ethylene glycol) monovinyl ether, maleic anhydride, obtained by a plasma-enhanced chemical vapour deposition (PECVD) [4–8], at low-pressure conditions, are quite suitable for the chemical functionalization of a sensing surface [9, 10], owing to the following reasons: (i) they do not change the chemical properties of the bulky material of a sensing device so leaving unaffected its working principle; (ii) they are conformal and (iii) do not need particular chemistry exposed to the sensor surface for adhesion; and (iv) they can show different features in terms of density of functional groups, wettability (hydrophilicity/hydrophobicity) and chemical stability by simply varying the process parameters (modulation of the plasma discharge, monomer or mixture of monomers/process gas, reactant vapour partial pressure, etc.), even though the same reagent is used as precursor (acrylic acid, vinyl acetic acid, allyl alcohol, allylamine) [11–13].

The chemical stability, in aqueous solution or other solvents (according to the biological protocol/technological procedure), is one of the mandatory goal to achieve, dealing with the plasma polymers exposing monotype functional groups suitable for covalent binding, as reported for polyacrylic acid and polyallylamine [14–19]. To enhance this last aspect, plasma copolymerization can be adopted to better tune the distribution and density of functional groups by mixing the monomer containing the functional groups (e.g. acrylic acid, allylamine, allyl alcohol) of interest with a precursor which does not contain specific functionalities (e.g. ethylene, styrene) and which has the function to dilute the reactive groups at the surface [20]. This last kind of monomers can be used alone to get a plasma polymer with bio-antifouling properties so allowing, for reference purpose, the detection of a blank response entirely unaffected by unspecific adhesion of biological materials, as shown by Sardella et al. for surface micro-domains of plasma-polymerized polyacrylic acid and polyethylene oxide [21]. The described polymers are also compatible with microscale lateral patterning based on photolithography combined with multiple subsequent plasma deposition steps. [22]

Concerning high-performing sensors, such as gravimetric (microcantilevers) [23] or optical (Bloch surface waves (BSW)-based one-dimensional photonic crystals) [24–27] microdevices, the limited thickness of the functionalizing coating represents a crucial task to reach in order to avoid losses of sensitivity in the biodetection, as, for the first type, additional masses have to be minimized and, for the second type, the perturbation of refractive index at the surface of the sensing device has to be finely tuned.

In this work, the study, optimization and characterization will be presented of ultra-thin plasma polymers and copolymers obtained from the vapours of acrylic acid containing a carboxylic (−COOH) group and styrene (an aromatic molecule with a vinyl as substituent at the ring). A particular attention will be devoted to match specific and critical requirements,

http://dx.doi.org/10.5772/62899

such as low thickness and refractive index, high surface density of reactive groups, bio-antifouling properties where required, reproducibility, and chemical resistance and stability.

Several plasma process conditions, amount ratio of the two kinds of precursors and thicknesses, ranging from 10 to 50 nm, were considered and the related coatings were characterized by means of OCA, ATR-FTIR, XPS and AFM. Through these techniques, it was possible to assess the chemical composition of the obtained films, the hydrophilicity and hydrophobicity, the effect of solvents on the chemical structure and thickness of coatings due to eventual dissolution.

The −COOH surface density of plasma-polymerized acrylic acid (PPAA) and copolymer (PPAA–ST) obtained by mixing styrene moieties to acrylic acid vapours during the plasma process was quantified by means of colorimetric titration through toluidine blue O (TBO) [28, 29].

Finally, the surface activity, towards test fluorophore-labelled proteins, versus binding or antifouling properties of the three selected polymers (PPAA, PPST and their copolymer) was studied by fluorescence microscopy.

2. Experimental

2.1. Chemicals

Pure acrylic acid, anhydrous, 99% (vapour pressure = 3.1 Torr at 20°C and 1 atm) and pure styrene, ≥99% (vapour pressure = 5 Torr at 20°C and 1 atm) liquid monomers, acetone, ACS reagent, ≥99.5% and acetic acid (glacial, ≥99%) were purchased by Sigma Aldrich. TBO (technical grade) and sodium hydroxide were obtained from Fluka. The AlexaFluor546-conjugated protein A (PtA-AF546) was purchased from Invitrogen. The phosphate buffer saline (PBS) 1× solution was from GIBCO®. All water solutions were prepared with Milli-Q™ grade water (Merk-Millipore, Milan).

2.2. Plasma polymerization system

Plasma treatments were carried out at room temperature in a low-pressure plasma-enhanced CVD reactor (chamber base pressure = 28 mTorr; RF = 13.56 MHz) purchased from IONVAC s.r.l., Rome, Italy [30]. The system is equipped with a delivery frame suitable to inject organic vapours coming from liquid reactants (monomeric precursors) stored in reservoirs intercepting the carrier gas lines.

The parameters of the plasma processes will be reported and discussed along the text in the Findings paragraph.

2.3. Characterization techniques

OCA measurements were used to investigate the surface properties of the differently functionalized samples in terms of hydrophilicity and hydrophobicity The OCAH 200 instrument

(DataPhysics Instruments GmbH), used for the characterization, is equipped with a charge-coupled device (CCD) camera and an automatic dosing system for the liquids. The selected ones for the sessile droplet method in static mode analysis (droplet volume = 1.5 μl) were deionized water MilliQ grade (H_2O) and diiodomethane (CH_2I_2, Sigma Aldrich). The Young–Laplace method was applied to fit the drop profiles and the SCA20 software was used to calculate contact angles between fitted function and base line. A data set of at least three droplets for each liquid was used to evaluate the standard deviation for each kind of sample.

ATR-FTIR spectra were collected in the range 4000–600 cm^{-1}, at 4 cm^{-1} resolution. Sixty-four scans were accumulated for each spectrum on a Nicolet 5700 FTIR spectrometer (ThermoFisher) equipped with a room temperature working deuterated triglycine sulphate (DTGS) detector and a diamond crystal ATR accessory.

A PHI 5000 Versaprobe scanning X-ray photoelectron spectrometer (monochromatic Al Kalpha X-ray source with 1486.6-eV energy) was employed to check the material surface chemistry. High resolution (pass energy: 23.5 eV) and survey spectra (pass energy: 187.85 eV) have been collected using a beam size of 100 μm. A combination of an electron gun and an Ar ion gun has been used as a neutralizer system to compensate the positive charging effect during the analysis, due to not perfectly conductive surfaces. Fitting procedure and deconvolution analysis have been done using the Multipak 9.6 dedicated software. All core-level peak energies were referenced to C1s peak at 284.5 eV (C–C/C–H sp^2 bonds).

AFM measurements were performed by the WiTec AlphaSNOM system that implements a combined AFM and scanning near-field optical microscopy (SNOM) in collection/illumination and scattering mode by employing microfabricated, hollow pyramidal probes. The profile step measurements by AFM module of the deposited plasma polymers were collected by tapping mode.

Wide-field fluorescence microscopy was performed by a LEICA DM-LM microscope (objective 20×) equipped with a Hg vapour arc lamp (50 W) and L5-type combination filters suitable for fluorescein-like fluorophore. The coated samples (Si and SiO_2) were incubated with a 0.1 mg/ml proteinA, Alexa Fluor 546 aqueous solution (dispensed volume = 10 μl) and rinsed in PBS, pH 7.3 + H_2O to remove unbounded protein.

Colorimetric titration of –COOH functionalities of PPAA and PPAA–ST films was performed by means of TBO. The amino group contained in TBO molecule reacts specifically with a surface carboxylic group according to a 1:1 ratio [28]. Functionalized samples (c-Si substrates were used) were contacted with 3 ml of 0.5 mM TBO aqueous solution (pH = 10) at 37°C, for 5 h, in the dark. Then samples were copiously rinsed with 0.1 mM NaOH solution to remove the unreacted dye. Afterwards, samples were transferred in 1.5 ml of 50% v/v acetic acid solution and shaken for 10 min, in order to completely release the TBO linked to the carboxylic functional groups. Colorimetric dosing of TBO (and consequently of carboxylic groups) was performed by using a 2100-C microplate reader (Ivymen Optic System), by recording the optical densities (OD) of the solutions recovered after the reaction with the samples at 630 nm. A solution of 50% v/v acetic acid was used as reference background. By applying the Lambert–Beer law to the OD recorded for the different samples, on the basis of the comparison with an

http://dx.doi.org/10.5772/62899

internal calibration obtained with TBO solutions (at known concentrations and volumes), and through the normalization for the geometric surface of the test samples, the evaluation of carboxylic functionalities density (in terms of groups/cm^2) can be performed.

In order to get information on the chemical characteristics of PPAA, PPST and PPAA–ST films, flat substrates, that is silicon (CZ/1-0-0, boron/P-type), Corning (Danville) glass and polyethylene (low-density PE; thickness 2.3 mm; Good Fellow) were used for the most of characterizations. For OCA, the different substrates were used in order to verify that the coating has the same properties without any dependence on substrate chemical composition, even for low thicknesses. For FTIR-ATR spectroscopy, silicon was not used owing to its refractive index higher than the ATR module diamond crystal. PE and Corning glass substrates have absorptions in different spectral range hiding thin film vibrational absorption features in different complementary parts of the selected range of spectra collection. The use of both substrates allows the investigation of the plasma polymer vibrational modes in the whole 400–4000 cm^{-t}. For XPS and AFM, only silicon was used.

3. Findings

3.1. Plasma polymerized acrylic acid

The advantages of using acrylic acid as a precursor for plasma polymerization are the quite low vapour pressure that makes controllable the flux of vapours by manual metering valve (calculated AA vapour flow was approximately of 3 sccm), the nearly absent toxicity of reactants, the presence of an unsaturation (vinylic double bond) allowing the radical polymerization mechanism and a carboxylic functionality (−COOH).

This chemical group is particularly suitable to biosensing applications because it forms easily amidic bridges by reacting with amino groups of biomolecules (e.g. receptor antibodies) with (binding efficiency is enhanced) or without further chemical activation.

In previous works of the authors [4, 26, 30, 31], films with thicknesses included between 80 and 120 nm (processes performed by T_{Dep} between 10 and 20 min) and prepared by means of both continuous wave (CW) and modulated wave (MW) plasma discharge were widely studied. The coating obtained by CW discharge were shown to not retain enough carboxylic functionalities while, among MW coatings, only the film obtained with an RF starting power of 200 W, a duty cycle of 0.1 with a t_{on} of 10 ms and a t_{off} of 90 ms with Ar as carrier gas, were optimal in terms of stability and reproducibility. A step of immersion in d-H_2O is required after plasma synthesis in order to remove surface oligomers (left at the end of plasma process) so making the film chemically stable for the following interaction steps (biosensing) in aqueous media. Moreover, to enhance the adhesion among the substrate and the deposited film an Ar plasma treatment was required before the film deposition. Thick films allowed a complete and reliable surface characterization that consisted of OCA, FTIR-ATR spectroscopy, XPS analysis, fluorescence microscopy, quartz microbalance system and colorimetric titration. By means of the last, an exceptional value of 1.15 ± 0.35 × 10^{16}groups/cm^2 was found. Moreover, from

ellipsometric characterization, it also aroused that the optimal film has a refractive index of 1.51 measured on 40-nm thick layers, after d-H_2O rinsing and from electrokinetic characterization based on the zeta (ζ) potential measurements, that allows the evaluation of acid–base properties, came that PPAA isoelectric point is at pH = 2.1. This indicates that the surface charge originates from the dissociation of the carboxylic acid groups of the PPAA chains and so from the deprotonation of –COOH species [4].

In the following, the characterization of PPAA ultra-thin films is reported in order to define the minimum thickness that can be reached without affecting the chemical resistance mainly in aqueous media and the functional group number and reactivity.

For these processes, Argon (Ar) is the AA vapour–carrier gas (flow =20 sccm). It is made bubble in liquid AA in order to enhance vapours formation and transport them into the chamber. The in-chamber total pressure in presence of the Ar–AA mixture is about at 220–240 mTorr, with a partial pressure of AA vapours of about 25 mTorr. The plasma parameters were an RF starting power of 200 W, a duty cycle of 0.1 with a t_{on} of 10 ms and a t_{off} of 90 ms.

After the film deposition, characterizations were performed before and after rinsing the substrates in de-ionized water (d-H_2O) for 20 min.

OCA angles performed on bare silicon (Si) and Corning glass with d-H_2O and CH_2I_2 (diiodomethane) and related calculation of surface energy (SE, W_{sl}) divided in its disperse (W^d_{sl})and polar (W^h_{sl}) components, are reported in **Table 1**.

Substrate	OCA_{H_2O} (deg)	$OCA_{CH_2I_2}$ (deg)	W_{sl} (mN/m)	W^d_{sl} (Watt)	W^h_{sl} (min)
Si	47 ± 1	46 ± 3	53,24	25,29	27,95
Corning	54 ± 1.5	38 ± 2	50,88	30,94	19,94

Table 1. OCA angles and SE data for bare substrates.

Time (min)	OCA_{H_2O} (deg)	$OCA_{CH_2I_2}$ (deg)	W_{sl}(mN/m)	W^d_{sl} (mN/m)	W^h_{sl} (mN/m)
2.5	15±1	34±2	70,89	27.17	43.72
4	11.3±0.9	35±1	71.80	26.56	45.24
5	17.1±0.8	32.3±0.5	70.41	28.24	42.17
7.5	15.6±0.2	31.2±0.4	70.98	28.63	42.35
10	15±1	34±2	70.94	27.20	43.74

Table 2. OCA angles and SE data for different PPAA films deposited at increasing T_{Dep} on c-Si.

Time (min)	OCA_{H_2O} (deg)	$OCA_{CH_2I_2}$ (deg)	W_{sl}(mN/m)	W^d_{sl} (mN/m)	W^h_{sl} (mN/m)
2.5	16.7 ± 0.4	36 ± 0	70.27	26.63	43.64
4	14.2 ± 0.6	35.0 ± 0.9	71.09	26.89	44.20

http://dx.doi.org/10.5772/62899

Time (min)	OCA_{H_2O} (deg)	$OCA_{CH_2I_2}$ (deg)	W_{sl}(mN/m)	W^d_{sl} (mN/m)	W^h_{sl} (mN/m)
5	17.4 ± 0.9	35 ± 2	70.09	26.99	43.10
7.5	17.2 ± 0.1	34.9 ± 0.4	70.18	27.14	43.04
10	16.6 ± 0.6	36 ± 2	70.26	26.33	43.92

Table 3. OCA angles and SE data for different PPAA films deposited at increasing T_{Dep} on Corning glass.

An example of the similar surface chemistry of PPAA at the lower T_{Dep} for both c-Si and Corning glass is reported in **Figure 1**. It also shows that any effect of substrate chemistry is absent. The high polar component of the surface energy (see **Tables 2** and **3**) confirms that the surface of the test substrates is homogeneously coated by polar hydrophilic species.

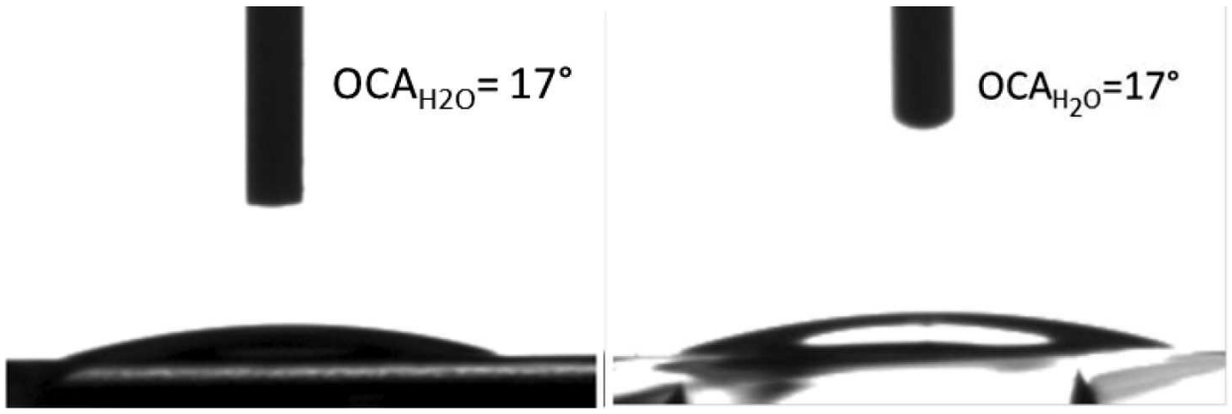

Figure 1. Example of OCA_{H_2O} on PPAA-2.5 min film on c-Si and on Corning.

The FTIR-ATR spectra of **Figure 2**, collected on both PPAA-deposited PE and Corning glass, confirm that the species exposed at surface are carboxylic groups and that they are also visible for the thinner film.

An effect of thickness growth is evident. The absorption features of –COOH groups increase according to the length of T_{Dep}: the band between 3750 and 3200 cm^{-1} assigned to the absorption envelope of O–H stretching mode, the C–H stretching mode at 2980–2870 cm^{-1} visible on Corning glass substrate, at 1730–1710 cm^{-1} the absorption related to C=O stretching, corresponding to both carboxylic and carbonyl functionality, the C–H bending mode at 1460–1370 cm^{-1} and the C–O stretching mode at 1200 cm^{-1} visible on PE substrates. The effects of rinsing in water are also visible (dotted curves) as a slight decrease of –COOH absorption features for higher thicknesses.

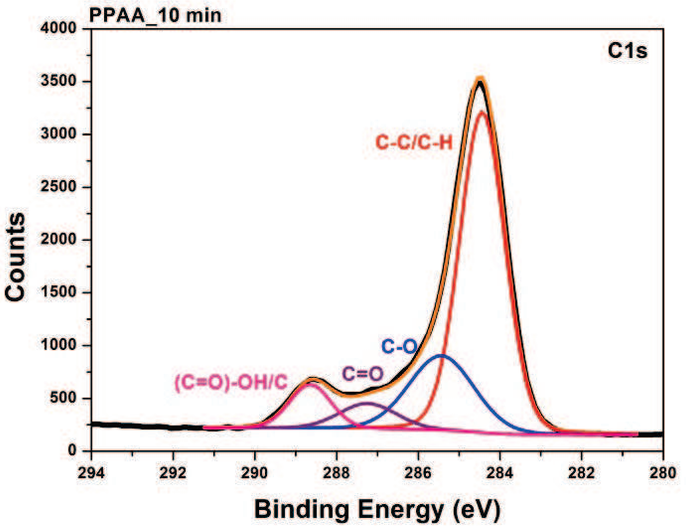

Figure 2. FTIR-ATR spectra measured on PE (a) and Corning glass (b) substrates coated with PPAA films obtained at increasing T_{Dep}.

XPS analysis (HR–C1s spectrum, reported in **Figure 3**) of the PPAA coating, deposited on c-Si, shows the C–C/C–H peak at 284.5 eV, a second intense component at 285.4 eV, assigned to C–O species, a third one at 287.3 eV related to C=O groups and a third component at 288.7 eV related to the (C=O)O–H/C species. All the features are consistent with the presence of carboxylic chemical groups and they will be used for the sake of comparison in the paragraph devoted to XPS analysis on PPAA–ST films.

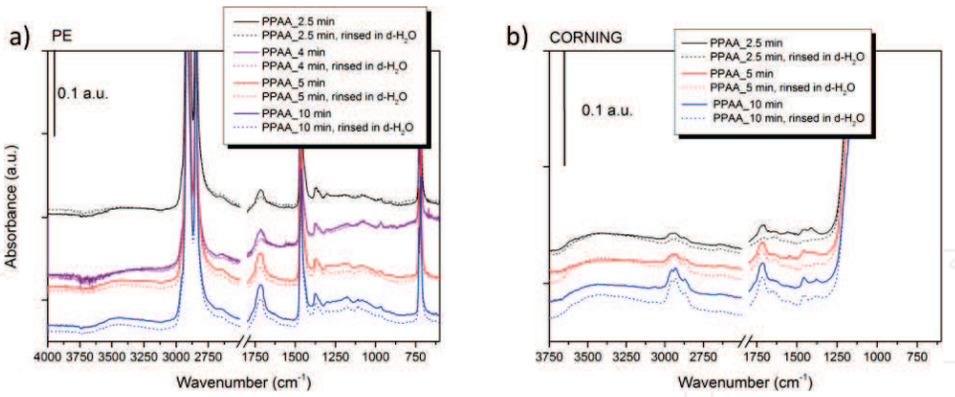

Figure 3. XPS analysis on PPAA obtained TDep of 10 min (C1s HR spectrum).

In the following, the correlation between T_{Dep} and film thickness in the range 0–50 nm was performed by means of AFM for profilometric purposes, in order to get a calibration of selected process and information about deposition rate.

From **Table 4** arises that the deposition rate has not a linear behaviour. For low times of deposition, the rate is not reproducible (several processes at the same deposition time were performed) due the starting step of pulsed discharge stabilization that is not controllable.

http://dx.doi.org/10.5772/62899

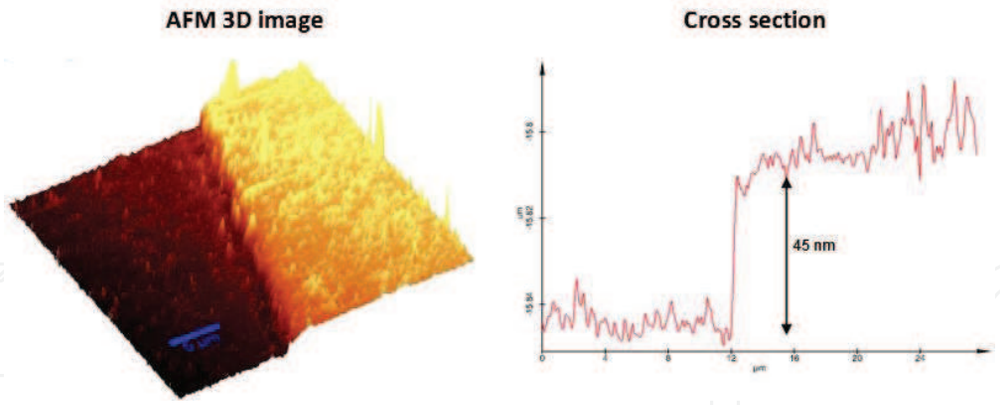

Figure 4. PPAA (T_{Dep} = 5 min) AFM characterization.

For this reason, the minimum deposition time allowing reproducible thicknesses is 4 min, that is a thickness of 40 nm.

Time dep (min)	Time dep (s)	Thickness (nm)	Dep rate (nm/s)	Dep rate (nm/min)
2.5	150.0	25.0	0.17	10
4	240.0	40.0	0.17	10
5 (Figure 4)	300.0	45.0	0.15	9
7.5	450.0	60.0	0.13	8
10	600.0	85.0	0.14	8.5

Table 4. AFM profilometry: PPAA thickness values at different deposition times.

3.2. Plasma-polymerized styrene

Styrene is an aromatic molecule (C_6H_6–CH=CH_4) which, by decomposing, during plasma process, and reassembling in form of cross-linked chains, allows to get a polymer with mechanical toughness, thermal stability, dielectric properties and chemical resistance/inertness. These properties make it a good bio-antifouling surface. Moreover, it can be used to dilute other functional monomers, thus allowing to introduce aliphatic fragments/aromatic rings among carboxylic groups arising from a chemically functional monomer, such as acrylic acid. A plasma copolymer can be so obtained, as reported in the next paragraph.

The explored processes, by changing different parameters such as the discharge mode (CW and MW), were performed at 2 and 10 min of deposition time. With respect to AA, the monomer flow, measured when the manual valve intercepting the reservoir is open, is not easily controllable and it is highly sensitive to external temperature variations. This could create problems for the reproducibility of the processes and does not allow the measure of the vapour flow of styrene as in the case of acrylic acid.

Process type	P_{RF} (Watt)	D.C.	t_{on} (ms)	t_{off} (ms)	P_{AVE} (Watt)
PPST_1	60	CW			
PPST_2	200	0.1	20	180	20
PPST_3	200	0.1	50	450	20
PPST_4	200	0.1	10	90	20
PPST_5	200	0.5	50	50	100

Table 5. PPST process parameters.

XPS analysis was carried out on selected spectra, obtained with time of deposition of 10 min, in order to confirm the presence of intact benzene ring and to evaluate the content of oxygen that, even if unwanted, seems to be embedded in the coatings (due to quite low vacuum produced by the chamber pumping system). This side effect is supported by data reported in literature.

The analysis has been performed on the MW-obtained coatings only. **Figure 5** reports the C1s HR spectrum (a) and the O1s HR spectrum (b) of process PPST_2 of **Table 5**, obtained at P = 200W; DC = 0.1; t_{on}/t_{off} = 20 ms/180 ms. Peaks have been deconvoluted using Gaussian–Lorentz functions, while backgrounds have been removed with Tougaard functions. Fitting peaks are:

- the lower energy peak (284.3 eV) has been assigned to ring carbons;,
- the peak at 284.5 eV has been attributed to the presence of C atoms linked as C–C/C–H,
- the peak at 285.5 eV is commonly attributed to C–O–C,
- the higher energy peak (~291 eV) is due to π–π^* transitions arising from the presence of the aromatic rings. It is called "shake-up" satellite because related to "shake-up" excitations taking place in the π orbitals on the benzene rings.

Concerning the O1s HR spectrum, only one fitting peak was found, related to C–O–C chemical bonds.

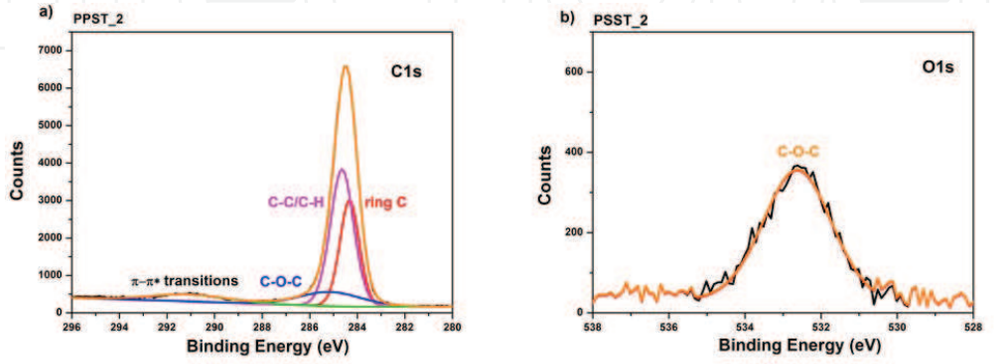

Figure 5. HR C1s spectrum (a) and HR O1s spectrum (b) of PPST_2.

http://dx.doi.org/10.5772/62899

The processes of the PPST_2 kind are the most reproducible, without a dependence on the deposition time, for this reason it is the most representative to single out the features of the HR C1s and O1s spectra of all the PPST processes.

For all processes, XPS peaks, in the energy range corresponding to valence band photoelectrons, are similar to that of a standard polystyrene. In fact, an extensive amount of information is also available from the valence band region. This is because the shifts in this region arise from changes in chemical bonding, rather than the chemical shifts caused by the environment found in the core region.

Process type	Dep time (min)	O/C atomic percentage ratio
PPST_1	10	0.07
PPST_2	2	0.05
PPST_2	10	0.04
PPST_3	10	0.04
PPST_4	10	0.02
PPST_5	10	0.04

Table 6. O/C atomic ratio referred to elements percentage obtained from survey spectra of PPST films.

From **Table 6** comes that for all processes the content of oxygen is quite negligible. **Figure 6a** shows that, for the most stable process in terms of water resistance, the energy band affected by the rinsing in water is the one relate to ring carbons, so suggesting that the chemical weakness of PPST is the cross-linking among the benzene rings. However, this effect does not affect the hydrophobic/antifouling properties of the PPST coating.

Figure 6b reports the intensity distribution of components of C1s spectrum of three selected processes (**Table 6**). The comparison puts in evidence that the process at t_{on}/t_{off} = 20/180 produces a higher amount of ring carbons with respect to the others.

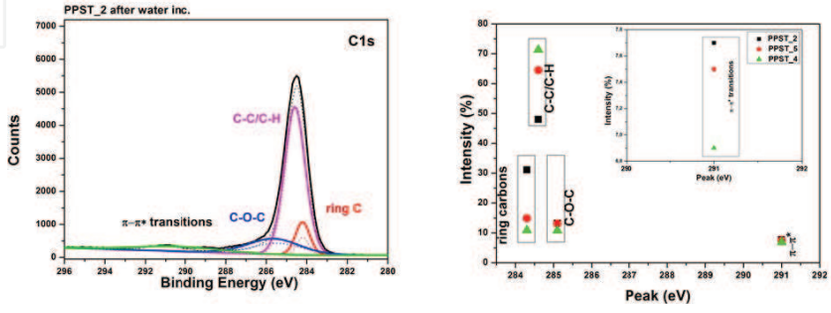

Figure 6. (a) Effects of water rinsing on component fitting peaks of HR-C1s spectrum of coating PPST_2 (dot line for water incubated sample, straight line for not-treated sample). (b) Intensity distribution of HR C1s components for sample PPST_2, PPST_4 and PPST_5 samples.

The process PPST_2 10 min; P = 200W; DC = 0.1; 20 ms/180 ms is the most performing in terms of low grade of oxidation, good retention of aromatic chemistry that ensures inertness and discourage electrostatic interaction.

To investigate on the bio-antifouling properties of it, it was deposited on the silica (SiO_2) surface of a glass substrate (a sector of the sample was masked) and incubated for 30 min with a solution of PtA labelled with a fluorescent marker (Alexa Fluor 546). After rinsing and drying under N_2 flux, according to the "Experimental" Section, the sample was observed by fluorescence microscopy.

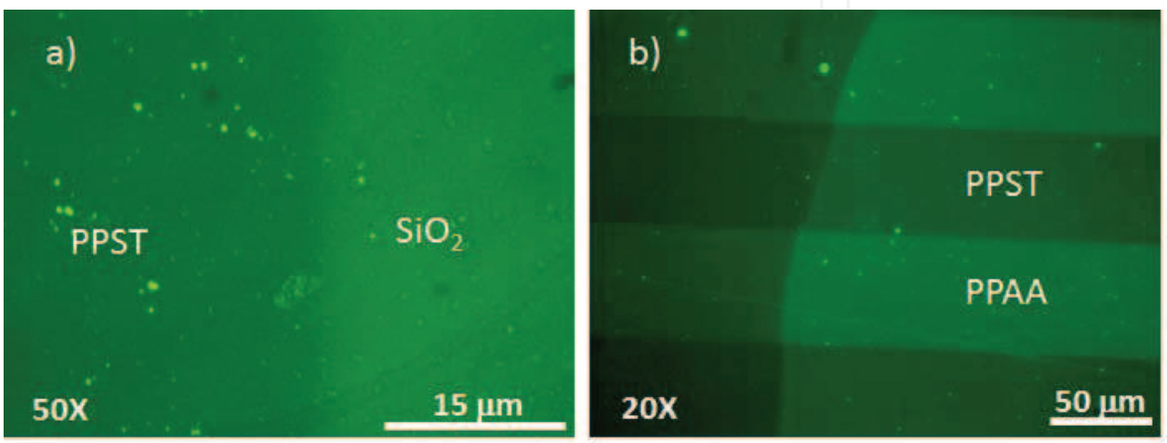

Figure 7. Fluorescence micrographs of PtA-Alexa Fluor 546 adhesion: (a) comparison between PPST film and bare SiO_2, (b) comparison between PPST and PPAA films.

It is evident from **Figure 7a** that selected PPST coating strongly limits unspecific adsorption of biomolecules, as fluorescent emission from PPST is lower or nearly absent with respect to the one coming from SiO_2. Moreover, concerning the lateral patterning involving PPST and PPAA is evident from **Figure 7b** that PPAA is highly PtA chemisorbing and PPST is bio-antifouling.

Also for PPST such as for PPAA is mandatory to verify that the compositional characteristics are retained also for thin layer. For this reason, the OCA measurements were performed on coatings obtained by different deposition time on the standard test substrates: Si and Corning glass.

The measured angles and related surface energies for coated Si and Corning substrates are reported in **Tables 7** and **8**, respectively. OCA_{H_2O} are quite high and confirm the hydrophobic properties of all the films. But a slight decrease of it is observed by incrementing the deposition time (here expressed in seconds). This trend suggests that longer is the deposition time, larger is the side oxidation effect produced by the process, and that is confirmed by FTIR-ATR spectra. Moreover, it is confirmed by the increase of the polar component of surface energy W^h_{sl}.

http://dx.doi.org/10.5772/62899

Time (s)	OCA_{H_2O} (deg)	$OCA_{CH_2I_2}$ (deg)	W_{sl} (mN/m)	W^d_{sl} (mN/m)	W^h_{sl} (mN/m)
15	77.2 ± 1.9	9.6 ± 0.8	50.15	47.11	3.04
120	77.3 ± 1	14.6 ± 0.8	49.27	46.1	3.17
240	76.5 ± 0.8	19.5 ± 1	48.15	44.43	3.72
600	72.8 ± 1.7	20.4 ± 0.9	48.52	42.86	5.66

Table 7. OCA and SE measurements performed on Si substrates coated with PPST films according to process PPST_2, at different deposition times.

Time (s)	OCA_{H_2O} (deg)	$OCA_{CH_2I_2}$ (deg)	W_{sl} (mN/m)	W^d_{sl} (mN/m)	W^h_{sl} (mN/m)
15	78.3 ± 0.9	21.4 ± 1.3	47.47	44.29	3.18
120	77.0 ± 1	14.2 ± 1.5	49.37	46.1	3.27
240	76.1 ± 1.3	16.3 ± 1.3	48.97	45.29	3.68
600	70.3 ± 1.7	17.1 ± 1.4	49.69	43.38	6.31

Table 8. OCA and SE measurements performed on Corning glass substrates coated with PPST films according to process PPST_2 at different deposition times.

OCA measurements were performed also on films after acetone rinsing, in view of photolithographic approaches for lateral patterning which involve the production of alternated chemical domains PPAA/PPST. OCA_{H_2O} slightly increases (see **Figure 8**) but the films chemically resists to the treatment.

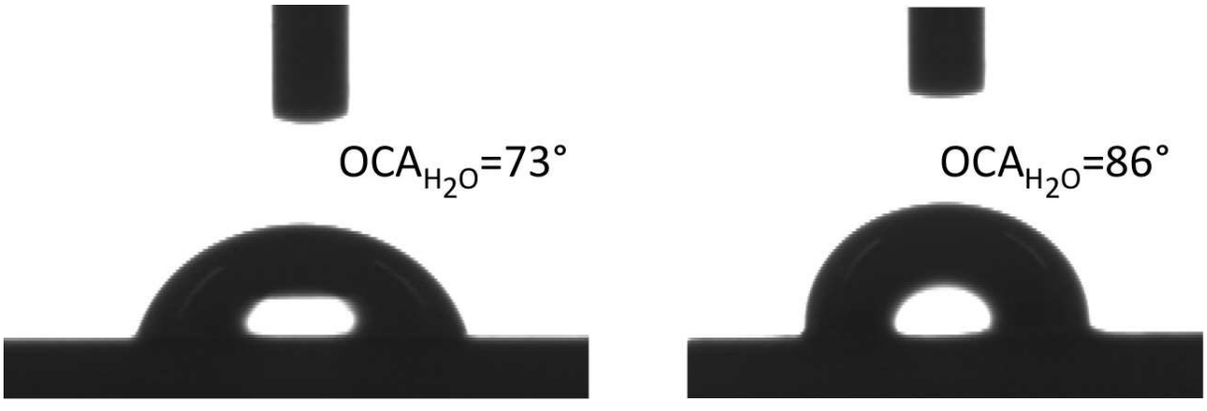

Figure 8. Comparison of OCA_{H_2O} on Si-PPST_2; P = 200 W; DC = 0.1; 20 ms/180 ms −600 s (10 min) process before (left) and after (right) rinsing in acetone.

The FTIR-ATR spectra of **Figure 9**, collected on the OCA characterized samples, on both PPST deposited PE and Corning, show the band associated to the C=C stretching in the aromatic ring at 1600 cm^{-1} and below 1200 cm^{-1}, the features due to the aliphatic backbone chain absorption modes. Most of spectra are present between 1730 and 1645 cm^{-1} absorption due to slight oxidation occurring during the process, and only for the thicker films, at 2980–2870 cm

$^{-1}$, the signals related to aliphatic C–H stretching mode are visible. An effect of thickness growth is observed as a slight increase of all described fingerprints. Finally, an effect of enhancement of aliphatic C–H stretching absorption, due to acetone rinsing is observed on the PPST_2-600s (10 min), coating (pink dashed curve), in accordance with OCA results (increase of hydrophobicity). Water rinsing seems to leave unaffected the PSST coating (related spectra are the dotted curves).

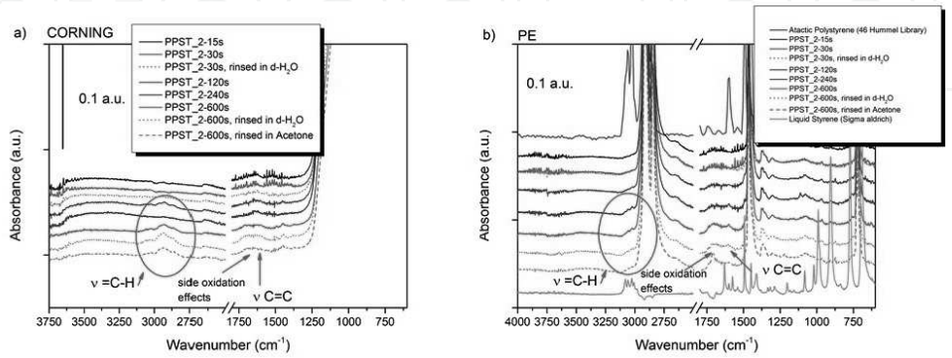

Figure 9. FTIR-ATR spectra measured on Corning (a) PE (b) substrates coated with PPST films obtained at increasing deposition time and compared with spectra of atactic standard polystyrene and liquid styrene.

In order to get a calibration of thicknesses of PPST in the lower range possible, according to deposition time, AFM was used with a profilometric approach and measured thicknesses are reported in **Table 9**.

Time dep (s)	Thickness (nm)	Dep rate (nm/s)	Dep rate (nm/min)
120	25.0	0.21	12.6
420	113.0	0.27	16.2

Table 9. AFM profilometry: PPST thickness values at different deposition times.

For T_{Dep} lower than 2 min, the rate is not reproducible due to the starting step of pulsed discharge stabilization that is not controllable. For this reason, the minimum deposition time allowing reproducible thicknesses is 120 s (2 min).

3.3. Copolymer

Plasma copolymerization is based on the activation of a plasma process in a gaseous mixture where the vapours of a monomer containing chemical active functionalities (acrylic acid) are mixed, in the reaction chamber, with the vapours of a chemically inert aliphatic chain/aromatic rings monomer, styrene, to achieve a sort of controlled "dilution" of the first in the second.

Thus, this mechanism allows to increase the film stability by lowering the number of carboxylic groups at surface and incrementing the cross-linking degree of the polymer in terms of backbone. Due to the higher reticulation, the film becomes more suitable for biological

http://dx.doi.org/10.5772/62899

applications where the sample has to be in contact with aqueous biological fluids for a long time. Some preliminary results were obtained [4] from ellipsometric and electrokinetics measurements. For the former, the high T_{Dep} copolymerized coating shows a thickness that is the double of that evaluated for the PPAA coating, obtained with the same discharge parameters and duty cycle. For the latter, the isoelectric point of the thick film (T_{Dep} = 7.5 min) obtained in the same operating conditions of PPAA–ST-1 (**Table 10**) was close to pH = 4, typical of inert surfaces.

Four kinds of processes (three in MW and one in CW mode), performed at the same T_{Dep} (5 min), are here below reported and characterized by means of OCA, ATR-FTIR and XPS analysis, in accordance to the parameters optimized for PPAA and PPST and by taking advantage from the previous preliminary copolymerization attempts.

Process type	P_{fwd} (W)	DC	t_{on} (ms)	t_{off} (ms)	P_{AA} (mTorr)	P_{STY} (mTorr)	P_{pro} (mTorr)	Ar_{AA} (sccm)	Ar_{STY} (sccm)
PPAA–ST_1	200	0,1	10	90	25	3	141–150	10	10
PPAA–ST_2	200	0,5	50	50	24	4	141–154	10	10
PPAA–ST_3	200	0,1	20	180	26	4	139–149	10	10
PPAA–ST_4	50	\	\	\	25	4	139–150	10	10

Table 10. Process parameters for plasma copolymerization of acrylic acid and styrene.

Concerning OCA characterization, OCA results of PPAA–PPST films deposited on Corning and silicon substrates are reported, respectively, in **Tables 11** and **12**.

Process type	OCA_{H_2O} (deg)	$OCA_{CH_2I_2}$ (deg)	W_{sl} (mN/m)	W^d_{sl} (mN/m)	W^h_{sl} (mN/m)
PPAA–ST_1	63 ± 2	28.6 ± 0.5	49.15	37.12	12.03
PPAA–ST_2	65 ± 0.5	28.1 ± 0.8	48.37	38	10.37
PPAA–ST_3	18.3 ± 0.7	32.9 ± 0.6	69.98	28.10	41.87
PPAA–ST_4	70.2 ± 0.9	16 ± 2	49.92	43.68	6.25

Table 11. OCA measurements performed on Corning glass substrates coated with PPAA–ST films obtained by plasma-copolymerization processes.

Process type	OCA_{H_2O} (deg)	$OCA_{CH_2I_2}$ (deg)	W_{sl} (mN/m)	W^d_{sl} (mN/m)	W^h_{sl} (mN/m)
PPAA–ST_1	63 ± 1	26.3 ± 0.8	49.7	38.17	11.53
PPAA–ST_2	66.4 ± 0.3	29 ± 2	47.77	38.16	9.61
PPAA–ST_3	15.3 ± 0.7	30.4 ± 0.2	71.14	28.92	42.21
PPAA–ST_4	66 ± 1	25.5 ± 0.6	48.79	39.29	9.50

Table 12. OCA measurements performed on Si substrates coated with PPAA–ST films obtained by plasma-copolymerization processes.

OCA values highlights an hydrophobic behaviour: by comparing OCA results of PPAA–ST copolymers with results of **Tables 2** and **3**, related to PPAA on silicon and Corning glass, respectively, it is clear that OCA_{H2O} values of PPAA–ST films are higher owing to the presence of the styrene component. The only exception is PPAA–ST_3 process. In **Figure 10** are shown the images of main OCA_{H_2O} contact angle related to PPAA–ST_1, PPAA–ST_2 and PPAA–ST_3 processes of **Table 10**.

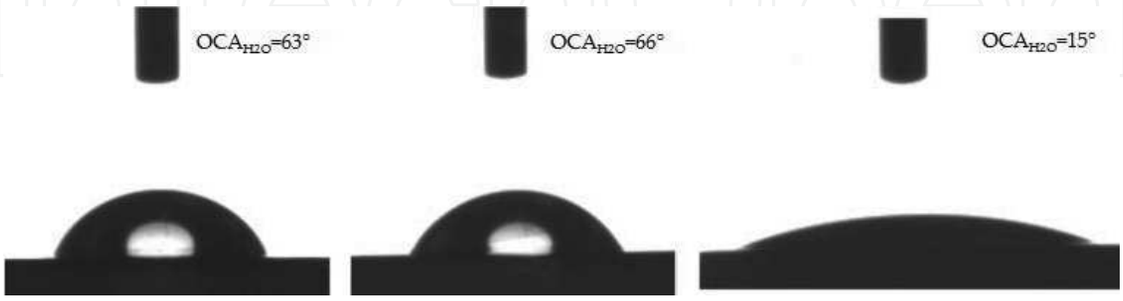

Figure 10. OCA_{H_2O} images for the first three processes listed in **Table 12**, on Si.

FTIR-ATR spectra related to processes listed in **Table 10** are reported in **Figure 11**.

As observed in **Figure 11**, spectra related to plasma copolymers reveal a sum of the features of both the reference polymers (PPAA and PPST). In particular, the spectrum of the film obtained with a t_{on}/t_{off} = 50/50 show characteristics similar to pure PPST. The others, except for the lower intensity of the signals related to the O–H and C=O stretching vibrations, show all the spectral features of carboxylic functionalities of pure PPAA.

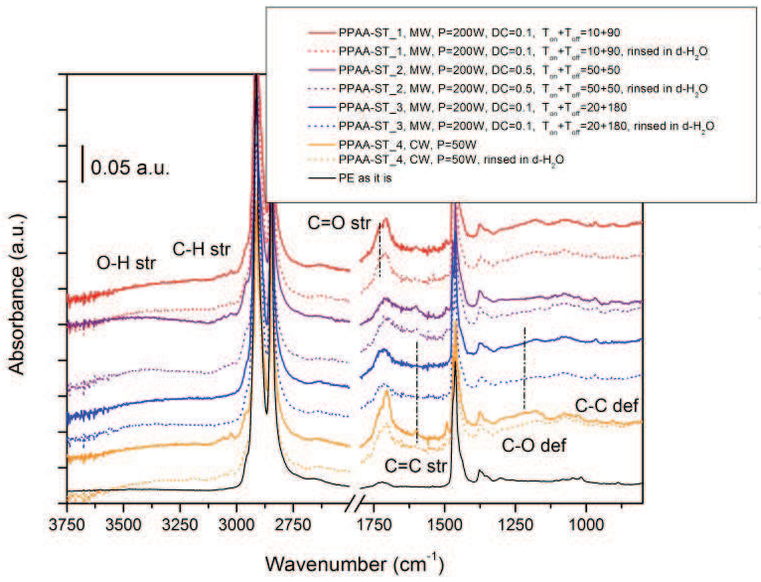

Figure 11. ATR FT-IR spectra measured on PE substrates coated with PPAA–ST copolymerized films, obtained by 7.5 min of deposition.

http://dx.doi.org/10.5772/62899

Under water rinsing, the most show good chemical resistance (except PPAA–ST_4). Under acetone rinsing, only the t_{on}/t_{off} = 50/50 process (PPAA–ST_2) is not dissolved (not shown).

Finally, XPS analysis was carried out in order to evaluate the chemical nature of the resulting copolymers (PPAA–ST): to get the evidence of both benzene rings/aliphatic chain presence and carboxylic functionalities at different grade of ratio. The analysis has been performed on the MW-obtained coatings only, listed in **Table 10**.

Figure 12 reports the C1s HR spectrum (a) and the O1s HR spectrum (b) of process PPAA–ST_2. Peaks have been deconvoluted using Gaussian–Lorentz functions, while backgrounds have been removed with Tougaard functions. Fitting peaks are:

- The lower energy peak (284.3 eV) has been assigned to ring carbons,
- The peak at 284.5 eV has been attributed to the presence of C atoms linked as C–C/C–H,
- The peak at 285.9 eV is commonly attributed to C–O–C/C–O–H,
- The peak at 288.6 is commonly attributed to COOH, O–C=O,
- The higher energy peak (~291 eV) is due to π–π^* transitions arising from the presence of the aromatic rings,
- The peak at 532.2 eV is attributed to C–O–C,
- The peak 533.5 eV is commonly attributed to COOH/C=O.

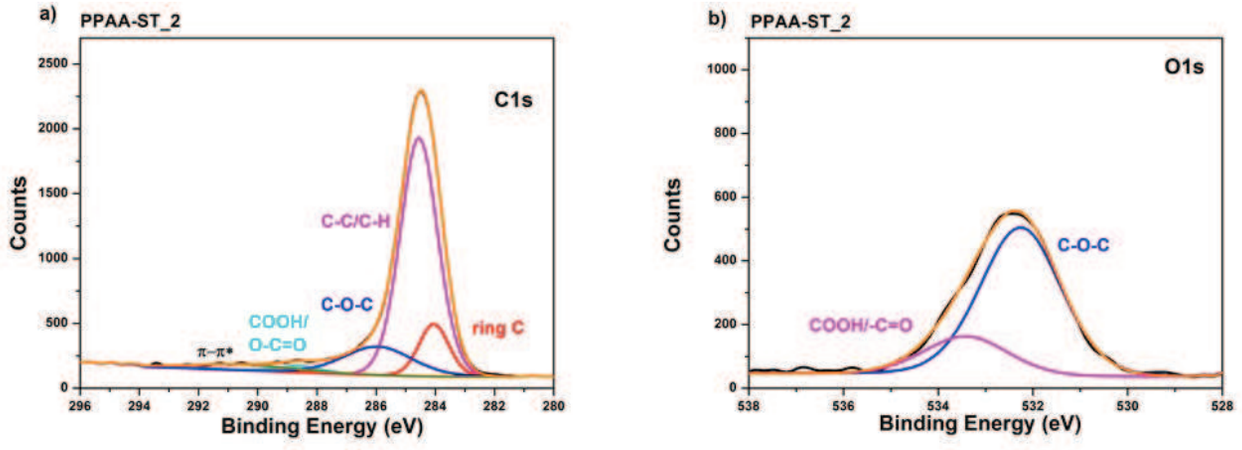

Figure 12. HR C1s spectrum (a) and HR O1s spectrum (b) of PPAA–ST_2 process (DC = 0.5 and t_{on}/t_{off} ratio = 50/50).

For process PPAA–ST_2, the C1s component related to π–π^* transition is higher than in spectrum related to process PPAA–ST_3 performed by a different DC and t_{on}/t_{off} ratio (0.1 and 20/180). In this last (**Figure 13**), all the components, of both HR C1s and HR O1s, are related to the higher embedding of acrylic acid species during chain propagation.

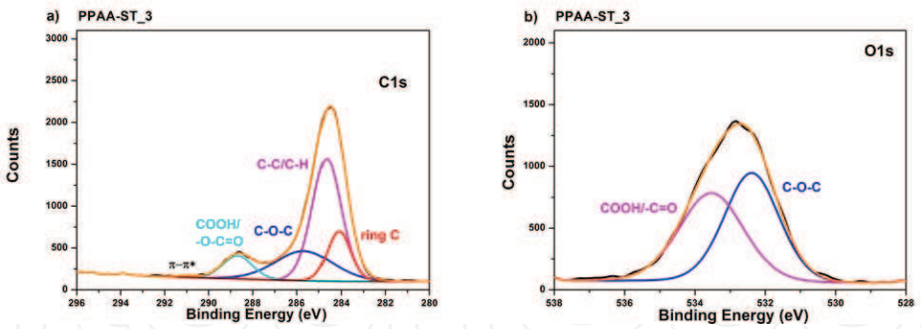

Figure 13. HR C1s spectrum (a) and HR O1s spectrum (b) of PPAA–ST process (PPAA–ST_3) at *P* = 200W; DC = 0.1; 20ms/180ms.

The comparison of all HR-C1s spectra (**Figure 14**) shows that the content of carbon and related components are different each other, as function of processes parameters. In particular, after rinsing of PPAA–ST_2 sample in acetone (spectrum PPAA–ST_2I), a little part of π–π^* transition component is lost and the carboxylic component increases, but this is the only kind of tested coating that quite resists to acetone treatment (in view of the photolithographic process for lateral patterning).

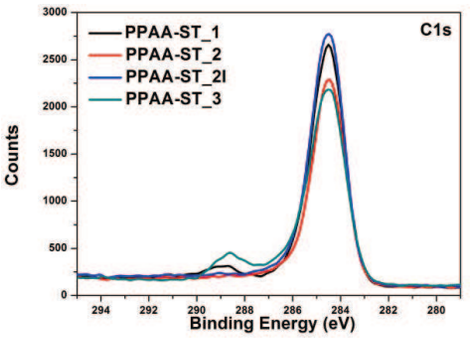

Figure 14. Comparison of HR C1s spectra for the first three processes listed in **Table 10**.

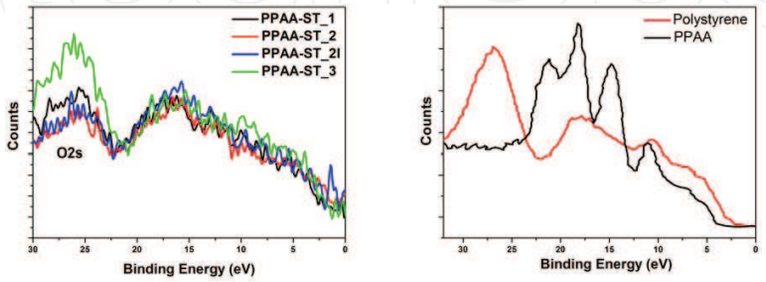

Figure 15. Comparison between all PPAA–ST processes valence band (left) HR spectra and reference valence bands spectra of polystyrene and a plasma-polymerized acrylic acid, reported in literature [32, 33] (right-image re-plotted by authors).

http://dx.doi.org/10.5772/62899

Notwithstanding evident differences among the spectra, all of them are quite consistent, in the low energy range of valence band, with the literature reference for plasma-polymerized acrylic acid, as shown in **Figure 15** (red spectrum in the graph on the left).

The trend of O/C ratio (**Table 13**) confirms that the process, producing a higher amount of oxygen-containing species (−COOH groups), is the PPAA–ST_3 and the most PPST-like one is the PP PPAA–ST_2 process.

Process type	Dep time	PPST films	O/C atomic percentage ratio
PPAA-ST_1	7.5 min	P = 200W; DC. 0.1; 10ms/90ms	0.16
PPAA-ST_2	7.5 min	P = 200W; DC. 0.1; 50ms/50ms	0.11
PPAA-ST_2I	7.5 min	P = 200W; DC. 0.1; 50ms/50ms + 5′ in acetone	0.10
PPAA-ST_3	7.5 min	P = 200W; DC. 0.1; 20ms/180ms	0.25

Table 13. O/C atomic ratio referred to elements percentage obtained from survey spectra of PPAA–ST films.

A colorimetric titration with TBO has been performed on PPAA–ST coatings deposited on Si according to different process parameters, after H_2O rinsing. Through this approach, it is possible to quantitatively estimate the surface density of –COOH groups exposed at the film surface and available for biomolecules grafting.

Table 14 reports surface density data obtained for several processes performed in CW and MW modes, on Si substrates. The results match the outcomes of previous characterizations: for DC = 0.5, the content of carboxylic reacting groups is under technique limit of detection, while for DC = 0.1 and CW process, the content is comparable with PPAA carboxylic groups density and so promising for biomolecules grafting.

Process type	Processes parameters	N°COOH/cm^2
PPAA–ST_1	Si-MW P_{ave} = 20 W; DC = 10%; t_{on} = 10 ms, t_{off} = 90 ms; Ar Etch	~5 × 10^{15}
PP AA-ST_2	Si-MW P_{ave} = 4 W; DC =50%; t_{on} = 50 ms, T_{off} = 50 ms; Ar Etch	0
PP AA-ST_3	Si-MW P_{ave} = 20 W; DC = 10%; t_{on} = 20 ms, t_{off} = 180ms; Ar Etch	~3 × 10^{15}
PP AA-ST_4	Si-50 W; Ar Etch	~4 × 10^{15}

Table 14. Carboxylic group density for plasma processes of Table 10.

In order to get a calibration of thicknesses of PPAA–ST in the lower range possible, already reported for PPAA (10–50 nm) according to deposition time, AFM was used with a profilometric approach.

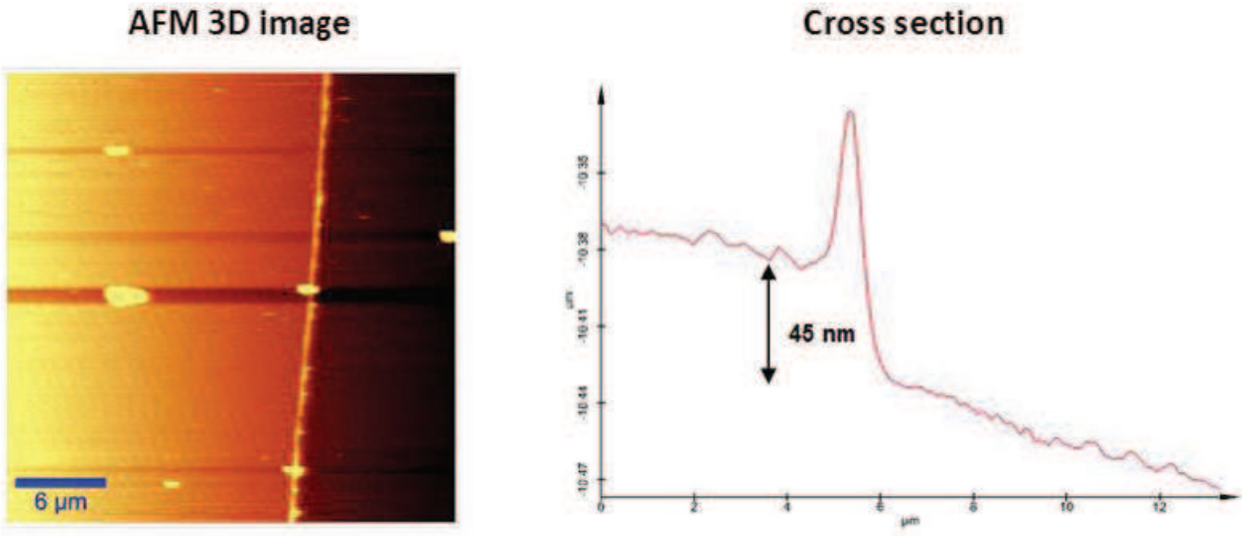

Figure 16. PPAA–ST_2 (T_{dep} =30 s) AFM characterization.

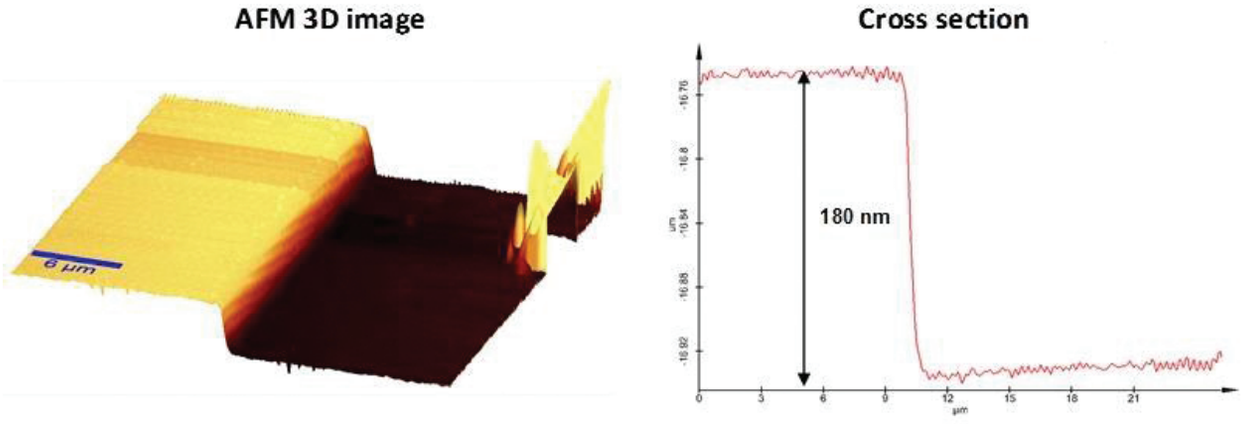

Figure 17. PPAA–ST_2 (T_{dep} = 5 min) AFM characterization.

PPAA–ST_2: DC 50% (t_{on} 50 ms t_{off} 50 ms) P = 200 W				
Time dep (min)	**Time dep (s)**	**Thickness (nm)**	**Dep rate (nm/s)**	**Dep rate (nm/min)**
0.5 (Figure 16)	30.0	45.0	1.50	90
1	60.0	80.0	1.33	80
5 (Figure 17)	300.0	180.0	0.60	36

Table 15. AFM measure: PPAA–PPST thickness values at different deposition time.

From **Table 15** arises that the deposition rate has not a linear behaviour and is dramatically huge with respect the other plasma polymers. The same behaviour is observed for the other processes of **Table 10**.

http://dx.doi.org/10.5772/62899

For PPAA–ST, the minimum deposition time possible, providing about 40-nm thick coatings, is 30 s, but this is quite uncontrollable due to the starting step of stabilization occurring when pulsed plasma discharge is activated.

4. Conclusions

In this work, the reliability to obtain, through a methodic approach, ultra-thin plasma polymerized coatings, about 40-nm thick, able to retain the chemical properties of the pristine precursor, for PPAA and PPST, in terms of binding and bio-antifouling, respectively, notwithstanding the quite low thickness and thus the short extension of macromolecular cross-linking in Z direction. PPAA coatings expose accessible carboxylic groups at a different grade of surface density (up to about 10^{16} –COOH groups/cm^2) and are stable in several aqueous media. The most performing PPST coating, with hydrophobic and so antifouling properties (that discourage proteins adsorption), resists also to solvent immersion, such as acetone.

Finally, an ultra-thin plasma copolymer, PPAA–ST, that merges the properties of PPAA and PPST was developed in order to enhance chemical stability of the chemically functional coating by diluting hydrophilic carboxylic functionalities. Moreover, the introduction of a higher content of aliphatic/aromatic components provided the reinforcement of the coating carbon backbone.

It is worth of note that, for a particular AA/ST ratio (PPAA–ST_1 process with DC = 10%; t_{on} = 10 ms, t_{off} = 90 ms), notwithstanding the increase in aliphatic fragments/aromatic rings content and thus in chemical resistance, the number of carboxylic groups exposed at the surface was shown to be only one order of magnitude lower than the one obtained for PPAA.

Acknowledgements

This research has received funding from the project BILOBA (no. 318035) granted in the frame of EU FP7/2007–2013 Programme. The authors thank Dr Mirko Nietschke (Institute für Polymer Vorschung, Dresden, Germany) for the support for the ellipsometric and electrokinetics measurements.

Author details

Paola Rivolo[1*], Micaela Castellino[2], Francesca Frascella[1] and Serena Ricciardi[1]

*Address all correspondence to: paola.rivolo@polito.it

1 Department of Applied Science and Technology, Politecnico di Torino, Turin, Italy

2 Centre for Space Human Robotics, Istituto Italiano di Tecnologia, Turin, Italy

References

[1] Muguruma H. Plasma polymerized films for biochips design. Plasma Processes and Polymers. 2010;7(2):151–162. DOI: 10.1002/ppap200900125

[2] Hessner M.J., Meyer L., Tackes J., Muheisen S., Wang X. Immobilized probe and glass surface chemistry as variables in microarray fabrication. BMC Genomics. 2004;5(1):53–61. DOI: 10.1186/1471-2164-5-53

[3] Cretich M., Damin F., Pirri G., Chiari M. Protein and peptide arrays: Recent trends and new directions. Biomolecular Engineering. 2006;23(2–3):77–88. DOI: 10.1016/j.bioeng.2006.02.001

[4] Ricciardi S. Surface chemical functionalization based on plasma techniques. Germany: LAP Lambert Academic Publishing; 2012. 236 p. ISBN-13: 978–3659190117

[5] Zhang Z., Menges B., Timmons R.B., Knoll W., Förch R. Surface plasmon resonance studies of protein binding on plasma polymerized di(ethylene glycol) monovinyl ether films. Langmuir. 2003;19(11):4765–4770. DOI: 10.1021/la026980d

[6] Liu S., Vareiro M.M., Fraser S., Jenkins A.T. Control of attachment of bovine serum albumin to pulse plasma-polymerized maleic anhydride by variation of pulse conditions. Langmuir. 2005;21(19):8572–8575. DOI: 10.1021/la051449e

[7] Detomaso L., Gristina R., Senesi G.S., d'Agostino R., Favia P. Stable plasma-deposited acrylic acid surfaces for cell culture applications. Biomaterials. 2005;26(18):3831–3841. DOI: 10.1016/j.biomaterials.2004.10.011

[8] Mourtas S., Kastellorizios M., Klepetsanis P., Farsari E., Amanatides E., Mataras D., et al. Covalent immobilization of liposomes on plasma functionalized metallic surfaces. Colloids Surface B: Biointerfaces. 2011;84(1):214–220. DOI: 10.1016/j.colsurfb.2011.01.002

[9] Kizling M., Järås S.G. A review of the use of plasma techniques in catalyst preparation and catalytic reactions. Applied Catalysis A: General. 1996;147(1):1–21. DOI: 10.1016/S0926-860X(96)00215-3

[10] Denes F.S., Manolache S. Macromolecular plasma-chemistry: An emerging field of polymer science. Progress in Polymer Science. 2004;29(8):815–885. DOI: 10.1016/j.progpolymsci.2004.05.001

[11] Förch R., Chifen A.N., Bousquet A., Khor H.L., Jungblut M., Chu L.-Q., et al. Recent and expected roles of plasma-polymerized films for biomedical applications. Chemical Vapour Deposition. 2007;13(6–7):284–294. DOI: 10.1002/cvde.200604035

[12] Rinsch C.L., Chen X., Panchalingam V., Eberhart R.C., Wang J.-H., Timmons R.B. Pulsed radio frequency plasma polymerization of allyl alcohol: Controlled deposition of surface hydroxyl groups. Langmuir. 1996;12(12):2995–3002. DOI: 10.1021/la950685u

[13] Yasuda H., Hsu T. Some aspects of plasma polymerization investigated by pulsed R.F. discharge. Journal of Polymer Science: Polymer Chemistry Edition. 1977;15(1):81–97. DOI: 10.1002/pol.1977.170150109

[14] Jafari R., Tatoulian M., Morscheidt W., Arefi-Khonsari F. Stable plasma polymerized acrylic acid coating deposited on polyethylene (PE) films in a low frequency discharge (70 kHz). Reactive and Functional Polymers. 2006;66(12):1757–1765. DOI: 10.1016/j.reactfunctpolym.2006.08.006

[15] Finke B., Schröder K., Ohl A. Structure retention and water stability of microwave plasma polymerized films from allylamine and acrylic acid. Plasma Processes and Polymers. 2009;6(1):S70–S74. DOI: 10.1002/ppap.200930305

[16] Morent R., De Geyter N., Trentesaux M., Gengembre L., Dubruel P., Leys C., et al. Stability study of polyacrylic acid films plasma-polymerized on polypropylene substrates at medium pressure. Applied Surface Science. 2010;257(2):372–380. DOI: 10.1016/j.apsusc.2010.06.080

[17] Lin Y., Yasuda H. Hydrocarbon barrier performance of plasma-surface-modified polyethylene. Journal of Applied Polymer Science. 1996;60(12):2227–2238. DOI: 10.1002/(SICI)1097-4628(19960620)60:12<2227::AID-APP21>3.0.CO;2–2

[18] Kelly J.M., Short R.D., Alexander M.R. Experimental evidence of a relationship between monomer plasma residence time and carboxyl group retention in acrylic acid plasma polymers. Polymer. 2003;44(11):3173–3176. DOI: 10.1016/S0032-3861(03)00217-9

[19] Anders A. Fundamentals of pulsed plasmas for materials processing. Surface & Coatings Technology. 2004;183(2–3):301–311. DOI: 10.1016/j.surfcoat.2003.09.049

[20] Swaraj S., Oran U., Friedrich J.F., Lippitz A., Unger W.E.S. Surface chemical analysis of plasma-deposited copolymer films prepared from feed gas mixtures of ethylene or styrene with allyl alcohol. Plasma Processes and Polymers. 2007;4(4):376–389. DOI: 10.1002/ppap.200600215

[21] Sardella E., Gristina R., Ceccone G., Gilliland D., Papadopoulou-Bouraoui A., Rossi F., et al. Control of cell adhesion and spreading by spatial microarranged PEO-like and pdAA domains. Surface & Coatings Technology. 2005;200(1–4):51–57. DOI: 10.1016/j.surfcoat.2005.02.063

[22] Ballarini M., Frascella F., De Leo N., Ricciardi S., Rivolo P., Mandracci P., et al. A polymer-based functional pattern on one-dimensional photonic crystals for photon sorting of fluorescence radiation. Optics Express. 2012;20(6):6703–6711. DOI: 10.1364/OE.20.006703

[23] Ricciardi C., Ferrante I., Castagna R., Frascella F., Marasso S.L., Santoro K., et al. Immunodetection of 17deestradiol in serum at ppt level by microcantilever resonators. Biosensors and Bioelectronics. 2013;40(1):407–411. DOI: 10.1016/j.bios.2012.08.043

[24] Ballarini M., Frascella F., Michelotti F., Digregorio G., Rivolo P., Paeder V., et al. Bloch surface waves-controlled emission of organic dyes grafted on a one-dimensional

photonic crystal. Applied Physics Letters. 2011;99(4):043302–043305. DOI: 10.1063/1.3616144

[25] Ballarini M., Frascella F., Enrico E., Mandracci P., De Leo N., Michelotti F., et al. Bloch surface waves-controlled fluorescence emission: Coupling into nanometer-sized polymeric waveguides. Applied Physics Letters. 2012;100(6):063305–063309. DOI: 10.1063/1.3684272

[26] Frascella F., Ricciardi S., Rivolo P., Moi V., Giorgis F., Descrovi M., et al. A fluorescent one-dimensional photonic crystal for label-free biosensing based on Bloch surface waves. Sensors. 2013;13(2):2011–2022. DOI: 10.3390/s130202011

[27] Descrovi E., Morrone D., Angelini A., Frascella F., Ricciardi S., Rivolo P., et al. Fluorescence imaging assisted by surface modes on dielectric multilayers. The European Physical Journal E. 2014;68(3):53–55. DOI: 10.1140/epjd/e2014-40530-0

[28] Chen J.-P., Chiang Y.-P. Surface modification of non-woven fabric by DC pulsed plasma treatment and graft polymerization with acrylic acid. Journal of Membrane Science. 2006;270(1–2):212–220. DOI: 10.1016/j.memsci.2005.11.015

[29] Blanchemain N., Aguilar M.R., Chai F., Jimenez M., Jean-Baptiste E., El-Achari A., et al. Selective biological response of human pulmonary microvascular endothelial cells and human pulmonary artery smooth muscle cells on cold-plasma-modified polyester vascular prostheses. Biomedical Materials. 2011;6(6):065003–065014. DOI: 10.1088/1748-6041/6/6/065003

[30] Ricciardi S., Castagna R., Severino S.M., Ferrante I., Frascella F., Rivolo P., et al. Surface functionalization by poly-acrylic acid plasma-polymerized films for microarray DNA diagnostics. Surface & Coatings Technology. 2012;207:389–399. DOI: 10.1016/j.surfcoat.2012.07.026

[31] Rivolo P., Severino S.M., Ricciardi S., Frascella F., Geobaldo F. Protein immobilization on nanoporous silicon functionalized by RF activated plasma polymerization of acrylic acid. Journal of Colloid and Interface Science. 2014;416:63–80. DOI: 10.1016/j.jcis.2013.10.060

[32] Way W.K., Rosencrance S.W., Winograd N., Shirley D.A. Polystyrene by XPS. Surf Science Spectra. 1993;2:67–70. DOI: 10.1116/1.1247712

[33] O'Toole L., Beck A.J., Short R.D. Characterization of plasma polymers of acrylic acid and propanoic acid. Macromolecules. 1996;29:5172–5177. DOI: 10.1021/ma9518417